



HAL
open science

Spontaneous mutations in a regulatory gene induce phenotypic heterogeneity and adaptation of *Ralstonia solanacearum* to changing environments

Anthony Perrier, Xavier Barlet, David Rengel, Philippe Prior, Stéphane Poussier, Stéphane Genin, Alice Guidot

► To cite this version:

Anthony Perrier, Xavier Barlet, David Rengel, Philippe Prior, Stéphane Poussier, et al.. Spontaneous mutations in a regulatory gene induce phenotypic heterogeneity and adaptation of *Ralstonia solanacearum* to changing environments. *Environmental Microbiology*, 2019, 21 (8), pp.3140-3152. 10.1111/1462-2920.14717 . hal-02936851

HAL Id: hal-02936851

<https://hal.inrae.fr/hal-02936851>

Submitted on 11 Sep 2020

HAL is a multi-disciplinary open access archive for the deposit and dissemination of scientific research documents, whether they are published or not. The documents may come from teaching and research institutions in France or abroad, or from public or private research centers.

L'archive ouverte pluridisciplinaire **HAL**, est destinée au dépôt et à la diffusion de documents scientifiques de niveau recherche, publiés ou non, émanant des établissements d'enseignement et de recherche français ou étrangers, des laboratoires publics ou privés.



Distributed under a Creative Commons Attribution - NonCommercial - NoDerivatives 4.0 International License

Spontaneous mutations in a regulatory gene induce phenotypic heterogeneity and adaptation of *Ralstonia solanacearum* to changing environments

Anthony Perrier ¹, Xavier Barlet,¹ David Rengel,¹ Philippe Prior,² Stéphane Poussier,³ Stéphane Genin¹ and Alice Guidot ^{1*}

¹LIPM, Université de Toulouse, INRA, CNRS, Castanet-Tolosan, France.

²UMR, Peuplements Végétaux et Bioagresseurs en Milieu Tropical, INRA, Saint-Pierre, Réunion, France.

³UMR, Peuplements Végétaux et Bioagresseurs en Milieu Tropical, Université de la Réunion, Saint-Pierre, Réunion, France.

Summary

An evolution experiment with the bacterial plant pathogen *Ralstonia solanacearum* revealed that several adaptive mutations conferring enhanced fitness in plants arose in the *efpR* gene encoding a regulator of virulence and metabolic functions. In this study, we found that an *efpR* mutant systematically displays colonies with two morphotypes: the type S ('smooth', similar to the wild type) and the type EV ('*efpR* variant'). We demonstrated that the *efpH* gene, a homologue of *efpR*, plays a key role in the control of phenotypic heterogeneity, the Δ *efpR*- Δ *efpH* double mutant being stably locked into the EV type. Using mixed infection assays, we demonstrated that the type EV is metabolically more proficient than the type S and displays fitness gain in specific environments, whereas the type S has a better fitness into the plant environment. We provide evidence that this *efpR*-dependent phenotypic heterogeneity is a general feature of strains of the *R. solanacearum* species complex and could occur in natural conditions. This study highlights the potential role of phenotypic heterogeneity in this plant pathogen as an adaptive trait to changing environments.

Introduction

In bacterial clonal populations, individual cells often harbour variation in their phenotype even when living in the same environment. The most common observation is variation in the morphology of colonies arising from single clones (Workentine *et al.*, 2013; Ronin *et al.*, 2017), but other phenotypic variations are also routinely observed such as antibiotic resistance, motility, growth profiles or biofilm formation (Chai *et al.*, 2008; Workentine *et al.*, 2013; Arnoldini *et al.*, 2014). The molecular mechanisms that lead to phenotypic heterogeneity in bacteria are very diverse and include phase variation, gene expression noise, post-transcriptional modification or epigenetic mechanisms (Hallet, 2001; Acar *et al.*, 2008; Veening *et al.*, 2008; Fraser and Kaem, 2009; Casadesús and Low, 2013). Phenotypic heterogeneity has been widely reported for bacterial pathogens with the description of co-existing virulent and avirulent (or less virulent) subpopulations (Diard *et al.*, 2013; Mouammine *et al.*, 2017; Ronin *et al.*, 2017; Chin *et al.*, 2018).

The development of heterogeneous subpopulations during host infection has been associated with various adaptive strategies (Ackermann, 2015; Weigel and Dersch, 2018). First, phenotypic heterogeneity can allow a genotype to survive in fluctuating environments (Rainey *et al.*, 2011; Schreiber *et al.*, 2016). For example, in *Salmonella*, heterogeneous expression of virulence factors allows a subset of the population to escape host inflammatory responses (Stewart *et al.*, 2011; Tuchscherer *et al.*, 2011). Another illustration of such bacterial bet-hedging strategy is the formation of 'persister' cells such as those resistant to antibiotics (Balaban *et al.*, 2004). A second adaptive explanation for phenotypic heterogeneity is the cooperation, or 'division of labour', strategy. Here, the phenotypically different sub-populations differentiate and cooperate to survive in non-fluctuating environments (Weigel and Dersch, 2018). Another possibility in isogenic subpopulation relationships involves the cell-to-cell variation in the production of public goods. Here, non-producing phenotypic variants behave like cheaters, which benefit from the subpopulation of producing cells without paying the metabolic costs (Strassmann, 2000; Harrison, 2013).

Received 28 January, 2019; revised 11 June, 2019; accepted 13 June, 2019. *For correspondence. E-mail alice.guidot@inra.fr; Tel. (+33) 05 61 28 55 92; Fax (+33) 05 61 28 50 61. This paper is dedicated to the memory of our wonderful friend and colleague, Philippe Prior, who passed away on November 11, 2018.

Very little is known about phenotypic heterogeneity of bacterial pathogens in non-mammalian hosts. The first example was reported for the plant pathogen *Pseudomonas syringae*, for which structural and regulatory components of the type 3 secretion system were shown to display heterogeneous expression within plant tissues (Rufián *et al.*, 2016, 2018). This bistable pattern of gene expression correlates with differences in virulence and is dependent upon complex regulatory loops, but the mechanism behind this phenomenon is not yet understood (Rufián *et al.*, 2016).

In an evolution experiment with the bacterial plant pathogen *Ralstonia solanacearum* (Guidot *et al.*, 2014), we observed the emergence of isogenic clones displaying phenotypic heterogeneity. *Ralstonia solanacearum* is the agent of bacterial wilt disease on more than 250 plant species around the world, mainly in tropical and sub-tropical countries (Mansfield *et al.*, 2012; Peeters *et al.*, 2013). This soil borne betaproteobacterium infects plants through the roots and invades the xylem vessels where it multiplies extensively, causing wilting symptoms and plant death. To identify determinants involved in host adaptation, experimental evolution of *R. solanacearum* was conducted by serial passage experiments from one plant to another during approximately 300 *in planta* bacterial generations in order to select for individuals with enhanced fitness (Guidot *et al.*, 2014). Interestingly, genome sequencing of such individuals revealed that single nucleotide polymorphisms (SNPs) appeared in a single gene, named *efpR*, in six independent lineages evolved on different hosts (Guidot *et al.*, 2014; Perrier *et al.*, 2016). *efpR* is a small gene (342 bp) encoding a transcriptional regulator and all but one SNPs identified were non-synonymous mutations. A reverse genetic approach confirmed that the SNPs detected in the *efpR* gene explained the fitness gain on plants (Guidot *et al.*, 2014; Perrier *et al.*, 2016). Further studies revealed that EfpR acts as a global catabolic repressor affecting several metabolic pathways; it also controls the expression of important virulence traits such as motility and the production of exopolysaccharides (EPS) (Perrier *et al.*, 2016; Capela *et al.*, 2017) and is therefore connected to the *R. solanacearum* virulence regulatory network (Peyraud *et al.*, 2016; 2018).

Here, we report that a *R. solanacearum* isogenic population carrying a mutation in the *efpR* gene systematically displays two different morphotypes of colonies on plates, thus revealing a phenotypic heterogeneity phenomenon. We investigated the functional relevance of such biological diversity generated through *efpR* mutations and its contribution to population dynamics *in planta* or in other environments. Importantly enough, a survey on *R. solanacearum* isolates from strain collections revealed that phenotypic heterogeneity behaviour can be detected among strains of the *R. solanacearum* species complex.

Results

Loss of function of efpR generates phenotypic heterogeneity

On complete medium plates supplemented with D-glucose and triphenyl tetrazolium chloride, the *R. solanacearum* wild-type (WT) strain GMI1000 forms fluidal and pink centered colonies (Fig. 1A). We observed that the *efpR* deleted mutant (Δ *efpR* strain) always produces two types of colonies on this medium: the first type is similar to the WT strain and was referred hereafter as type S (smooth), whereas the second type forming red, less mucoid colonies was designated type EV (*efpR* variant) (Fig. 1B). After subsequent subcultures, both isolated EV and S type colonies again systematically display colonies with the two morphotypes. This phenotypic heterogeneity phenomenon was observed for the Δ *efpR* strain but also for all the *efpR* SNP mutants that were selected during the evolution experiment *in planta* (Guidot *et al.*, 2014) (Supporting Information Fig. S1).

In a former study, we identified in the *R. solanacearum* genome a homologue of *efpR*, *RSc3149* hereafter named *efpH*, encoding for a putative transcription regulator having 79% protein identity with EfpR (Perrier *et al.*, 2016). We investigated whether this *efpR*-homologue also played a role in the advent of phenotypic heterogeneity observed with the Δ *efpR* strain. We generated a Δ *efpH* deletion strain and this strain had a WT S morphotype when plated on complete medium (Supporting Information Fig. S1). However, the Δ *efpR*- Δ *efpH* double mutant only formed EV type colonies (Fig. 1C and Supporting Information Fig. S1). The phenotype of the double mutant even appeared more pronounced than the Δ *efpR*-EV type with almost non-mucoid colonies at 52 h. However, after 72 h the *efpR*-EV colonies and Δ *efpR*- Δ *efpH* colonies looked similar. We never observed the occurrence of S type colonies from the Δ *efpR*- Δ *efpH* double mutant strain, suggesting that this strain is 'locked' into the EV morphotype.

S and EV morphotypes of the efpR mutants display specific gene expression patterns

To investigate the variation of gene expression occurring between the EV and S types, we constructed two transcriptional fusions with the respective promoters of *RSc3148* and *fliC* and the mCherry red fluorescent protein reporter gene. Both *RSc3148* and *fliC* genes were previously demonstrated to be among the top upregulated genes in the Δ *efpR* strain compared to the WT strain (Perrier *et al.*, 2016; Capela *et al.*, 2017). We found that in the S colonies formed by the Δ *efpR* mutant both promoters were either not expressed or expressed at a very low level, similarly to what happens in the S colonies formed by the WT strain

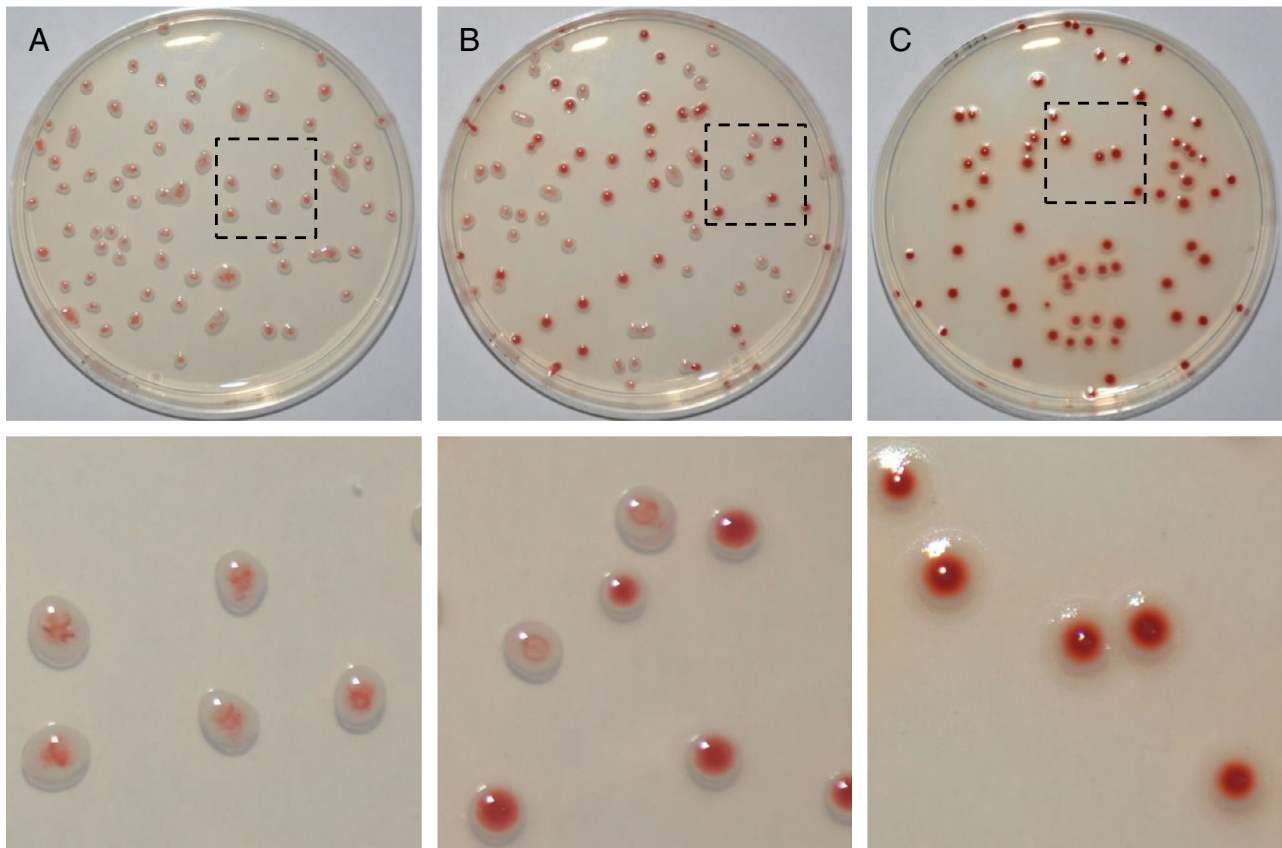


Fig. 1. *Ralstonia solanacearum* GMI1000 $\Delta efpR$ strain generates phenotypic heterogeneity. Colonies of the WT (A), $\Delta efpR$ (B) and the $\Delta efpR$ - $\Delta efpH$ (C) strains grown 52 h on complete medium agar plates supplemented with D-glucose and triphenyl tetrazolium chloride red. A zoom-in view corresponding to the dashed square zone is represented below each top-panel. The WT (S type) forms pink and fluidal colonies whereas the EV type appears as red and less mucoid colonies.

(Fig. 2 and Supporting Information Fig. S2). On the other hand, the *RSc3148* and *fliC* promoters were both strongly expressed in the EV colonies suggesting a specific expression pattern in EV colonies compared to the S ones (Fig. 2 and Supporting Information Fig. S2). As expected, in the colonies formed by the $\Delta efpR$ - $\Delta efpH$ mutant producing only EV colonies, the *RSc3148* and *fliC* promoters were strongly expressed in all the colonies (Fig. 2 and Supporting Information Fig. S2). Microscopic observations were also conducted at the cellular level to analyse the activity of the *fliC* promoter fused to a GFP reporter gene (Supporting Information Fig. S3). The analysis revealed that *fliC* is weakly expressed in WT strain cells (S type), highly expressed in $\Delta efpR$ - $\Delta efpH$ mutant cells (EV type) while in the *efpR* mutant (S + EV type), cells were either expressing *fliC* or not (residual expression).

Transcriptomic profiling confirms that the $\Delta efpR$ - $\Delta efpH$ double mutant is locked into the EV morphotype

To obtain a view of the global gene expression pattern in the EV morphotype, we examined the transcriptomic profiles of

the $\Delta efpR$ (EV colonies inoculum) and the $\Delta efpR$ - $\Delta efpH$ (EV) strains in comparison with the WT (S) during exponential growth in complete medium ($OD_{600nm} \sim 0.5$) (Supporting

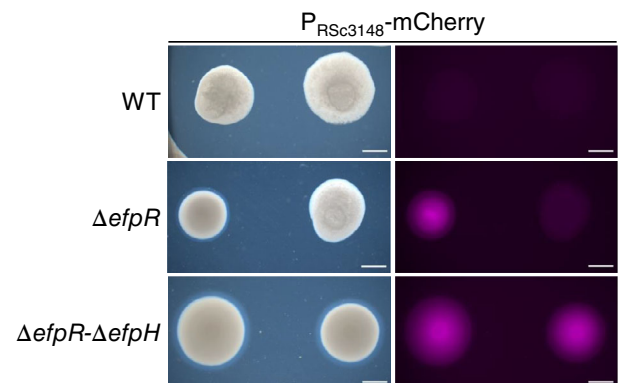


Fig. 2. Differential expression pattern of the *RSc3148* promoter in S and EV type colonies. Left panels show bright field images; the right panels show the same colonies under fluorescence excitation. For the $\Delta efpR$ strain, one type EV (left) and one type S (right) colonies are shown. Expression of the $P_{RSc3148}$ -mCherry reporter occurs only in EV type colonies. Bacteria were grown on complete medium agar plates for 72 h at 28°C. Scale bar = 2 mm.

Information Table S1). We found 674 (13.67%) differentially expressed genes (DEGs) (>twofold differentially expressed; p -value (p_{adj} , FDR) < 0.05) between the WT strain and $\Delta efpR$ strain, and 553 (11.22%) DEGs between the WT strain and the $\Delta efpR$ - $\Delta efpH$ strain (Supporting Information Table S2). In total, 743 genes were either differentially expressed in the $\Delta efpR$ -EV or the $\Delta efpR$ - $\Delta efpH$ mutants compared to the WT strain, with 484 DEGs shared by both strains, 190 specific to the $\Delta efpR$ strain and 69 specific to the $\Delta efpR$ - $\Delta efpH$ strain (Supporting Information Table S2). Comparison of the transcriptomes of the $\Delta efpR$ -EV strain with the $\Delta efpR$ - $\Delta efpH$ strain revealed only 25 DEGs (i.e. 0.51% of the expressed genes), indicating that the gene expression pattern was similar in both strains having an EV phenotype (Supporting Information Table S2). Among these 25 DEGs, 18 were downregulated in both strains compared to the WT strain including 12 genes belonging to the EPS biosynthesis cluster, 4 metabolism-related genes and 2 genes coding for a lectin and a putative transmembrane protein respectively. The observation that several EPS biosynthetic genes were more strongly repressed in the double mutant than in the single $efpR$ -EV mutant was in agreement with the more pronounced phenotype of the $\Delta efpR$ - $\Delta efpH$ double mutant on 52 h plates (less mucoid aspect, see Fig. 1C). Considering that (i) the transcriptomic profiles of the $efpR$ -EV type strain and the $\Delta efpR$ - $\Delta efpH$ double mutant largely overlap and (ii) the $\Delta efpR$ - $\Delta efpH$ was never observed to revert to WT phenotype, we concluded that the $\Delta efpR$ - $\Delta efpH$ is 'locked' into the EV morphotype.

The EV morphotype is strongly altered in pathogenicity

We previously showed that the $\Delta efpR$ mutant had reduced virulence on susceptible tomato plants compared to the WT

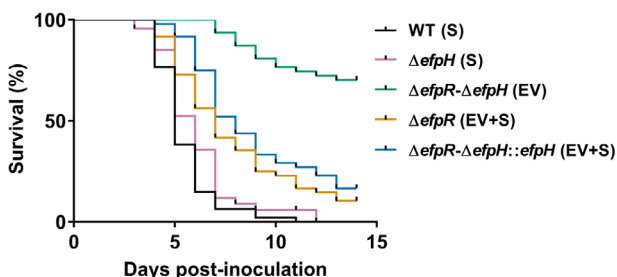


Fig. 3. Virulence of the EV type is strongly impaired on tomato. Kaplan–Meier survival analysis of tomato plants inoculated with the WT strain, the $\Delta efpR$ and the $\Delta efpH$ single mutants, the $\Delta efpR$ - $\Delta efpH$ double mutant and the $\Delta efpR$ - $\Delta efpH$:: $\Delta efpH$ complemented strain. The variant type (S or/and EV) found in the different genetic background is indicated in brackets. Curves represent three independent biological repeats of 15–16 plants inoculated by soil drenching. All the survival curves are significantly different from the WT survival curve (Gehan–Breslow–Wilcoxon test; $p < 0.0001$) except the survival curve of the $\Delta efpH$ single mutant (Gehan–Breslow–Wilcoxon test; $p = 0.0819$).

strain (Perrier *et al.*, 2016). Because the $\Delta efpR$ strain is phenotypically heterogeneous, we wanted to assess more accurately the respective contribution of the EV and S types to pathogenicity. We took advantage of the $\Delta efpR$ - $\Delta efpH$ double mutant as a stable EV type to evaluate its virulence on tomato plants. This double mutant was compared to the WT (type S), the $\Delta efpH$ strain (type S), the $\Delta efpR$ (type S + EV) strain, and the $\Delta efpR$ - $\Delta efpH$ double mutant complemented with the $efpH$ gene (type S + EV) (Fig. 3 and Supporting Information Fig. S1). The Kaplan–Meier survival analysis of tomato plants showed a significantly better survival for plants inoculated with all mutants compared to the WT strain, except for the $\Delta efpH$ mutant (Gehan–Breslow–Wilcoxon test; $p < 0.0001$), indicating that the presence of EV cells tends to decrease the disease symptom rate. The survival curve observed with the $\Delta efpR$ - $\Delta efpH$ strain showed that this double mutant was strongly altered for pathogenicity and significantly more than the $\Delta efpR$ strain (Gehan–Breslow–Wilcoxon test; $p < 0.0001$). On the other hand, the behaviour of the complemented strain ($\Delta efpR$ - $\Delta efpH$:: $efpH$) was not statistically different from the $\Delta efpR$ strain, indicating that the presence of a functional $efpH$ gene was able to restore phenotypic heterogeneity and so to increase the disease symptom rate on tomato (Fig. 3).

Fitness of the EV type is reduced in planta but increases in the presence of the S type

We compared the dynamic behaviour of the EV and S subpopulations *in planta* by conducting mixed infection assays of tomato plant stems. Because the $\Delta efpR$ mutant generates both EV and S types, in order to control the ratio of the EV and S types in our inoculums, we conducted these assays with the WT strain as the S type and the $\Delta efpR$ - $\Delta efpH$ strain as the EV type. Bacterial populations were recovered from stem sections 3 days after stem injection and the relative proportion of each strain quantified by GFP and mCherry fluorescent markers. This experiment first showed that the colonization of a homogeneous EV (EV+[EV]) population ($3.6 \pm 3.0 \times 10^8$ CFU g^{-1} FW) was strongly reduced compared to the homogeneous WT S (S+[S]) population ($1.8 \pm 0.79 \times 10^9$ CFU g^{-1} FW; p -value < 0.001, Kruskal–Wallis test with Dunn's post-test) (Fig. 4). In mixed populations, the S (S+[EV]) type had a significantly reduced colonization ($9.0 \pm 5.9 \times 10^8$ CFU g^{-1} FW; $p < 0.001$) compared to the homogeneous S (S+[S]) type reference, indicating that the EV type had a detrimental effect on the fitness of the S type (Fig. 4). However, monitoring the outcome of the EV subpopulation from a mixed infection with the S type (EV+[S]) revealed that co-infection was much beneficial for the EV type (reaching $2.5 \pm 1.7 \times 10^9$ CFU g^{-1} FW, statistically different when compared to the homogeneous EV (EV+[EV]) population; $p < 0.01$) (Fig. 4).

In order to rule out the possibility that the 1:1 initial infection ratio could induce a bias in the observed results, we performed similar co-inoculation experiments by varying the initial ratio of the mixed infection assay (100:0, 99:1, 90:10, 50:50 and 10:90). The obtained results showed that the S type population size from a **S+[EV]** mix started to decrease in the presence of only 1% of EV population (Supporting Information Fig. S4). It also confirmed that, conversely, the EV population size increased in presence of the S type (**EV+[S]**) (Supporting Information Fig. S4). We therefore concluded that the EV type is strongly compromised for *in planta* fitness but takes advantage from the presence of the S type to maximize its *in planta* growth.

The EV type could benefit *in planta* from the EPS produced by the S type

Ralstonia solanacearum secretes massive amounts of EPS *in planta*, where they act both as a colonization and a virulence factor (Genin and Denny, 2012). The EV type is strongly impaired in its capacity to secrete EPS, and so produces less mucoid colonies than the S type (Fig. 1). We hypothesized that EPS produced and secreted by the S type could be beneficial to the EV type, thus improving its ability for colonization *in planta*. To test this hypothesis, we introduced into the WT and the $\Delta\text{efpR}\text{-}\Delta\text{efpH}$ double mutant strains a $P_{\text{TAC}}\text{-xpsR}$ construct allowing the constitutive expression of *xpsR*, which is a positive regulator of the EPS biosynthetic genes (Huang *et al.*, 1995), acting independently of *efpR*. We investigated the virulence of the WT, the $\Delta\text{efpR}\text{-}\Delta\text{efpH}$ and the *xpsR*:: Ω strains bearing or not the $P_{\text{TAC}}\text{-xpsR}$ construct on susceptible tomato plants. The

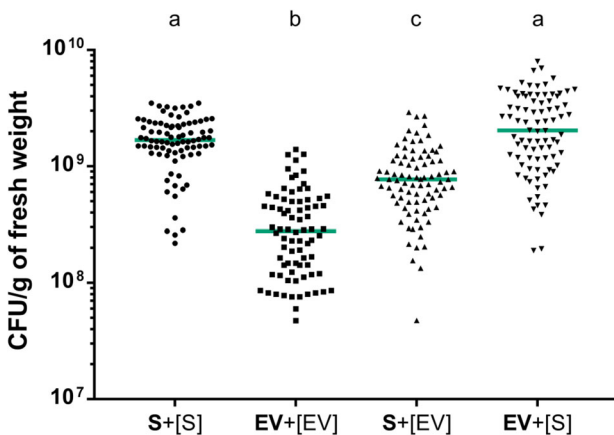


Fig. 4. *In planta* fitness of the EV and S types during co-infection. Bacteria were co-injected in tomato stems at a 1:1 ratio and harvested 3 days post-inoculation. Each dot represents the population size of the strain indicated in bold within a single plant after co-inoculation with the strain indicated in brackets. Horizontal bars indicate the median. Three independent biological repeats were performed with 10–18 plants per repeats per conditions. Kruskal–Wallis and Dunn’s multiple comparison test were used to establish statistical groups ($p < 0.001$). S = WT strain; EV = $\Delta\text{efpR}\text{-}\Delta\text{efpH}$ strain.

constitutive expression of *xpsR* in the $\Delta\text{efpR}\text{-}\Delta\text{efpH}$ and the *xpsR*:: Ω strains significantly improved their aggressiveness (Gehan–Breslow–Wilcoxon test; $p < 0.0001$) even if these two strains remained less aggressive than the WT strain (Gehan–Breslow–Wilcoxon test; $p < 0.0001$) (Fig. 5). These results therefore suggested that EPS produced by the WT (or S type) can rescue the EV type *in planta* to improve its colonization and virulence.

The EV type shows fitness gain in environments outside the plant

To investigate the behaviour of a mixed population (EV + S) in another environment than *in planta*, we performed an *in vitro* competition assay between the S (WT) and EV ($\Delta\text{efpR}\text{-}\Delta\text{efpH}$) types in complete medium and in minimal medium supplemented with different carbon sources (Fig. 6). Mixed populations with an initial 1:1 ratio between the EV and S types were cultivated in liquid minimal medium with a sole carbon source. The relative proportion of the EV and S types was then quantified when populations were up to 10^9 CFU ml^{-1} or above. In minimal medium, we found that the proportion of EV cells reached $75.6 \pm 5.4\%$ (L-histidine), $88.3 \pm 2.2\%$ (L-glutamine), $92.9 \pm 2.9\%$ (L-asparagine) and $96.3 \pm 1.3\%$ (L-proline), whereas in complete medium, the EV/S type ratio was close to 50% ($45.3 \pm 6.4\%$ of EV cells) (Fig. 6).

We then compared the growth dynamic of populations of the ΔefpR strain in liquid minimal medium + L-proline inoculated with a single colony of either the S or EV type (initial population corresponding to an $\text{OD}_{600\text{nm}}$ of 0.05). The culture inoculated with the $\Delta\text{efpR}\text{-EV}$ type reached a mean $\text{OD}_{600\text{nm}}$ of 1.0 after 40.9 h while it took 61.7 h to reach the same mean $\text{OD}_{600\text{nm}}$ for the one inoculated with the $\Delta\text{efpR}\text{-S}$ type in the same condition (Fig. 7). In comparison, the WT

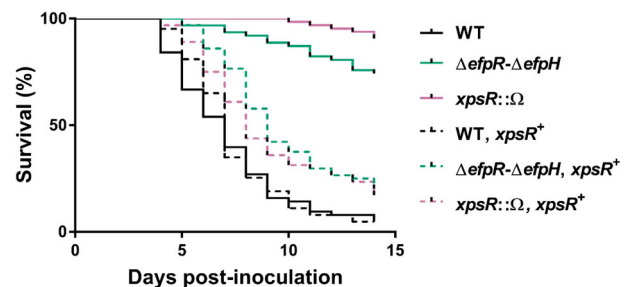


Fig. 5. Virulence of the EV type is partially restored by constitutive expression of *xpsR*, a positive regulator of *eps* genes. Kaplan–Meier survival analysis of tomato plants inoculated with the WT, the $\Delta\text{efpR}\text{-}\Delta\text{efpH}$ and the *xpsR*:: Ω strains with and without the $P_{\text{TAC}}\text{-xpsR}$ construct (*xpsR*⁺). Curves represent three independent biological repeats of 15–16 plants inoculated by soil drenching. All the survival curves are significantly different from the WT survival curve (Gehan–Breslow–Wilcoxon test, $p < 0.005$) except the survival curve of the WT, *xpsR*⁺ strain (Gehan–Breslow–Wilcoxon test; $p = 0.3637$).

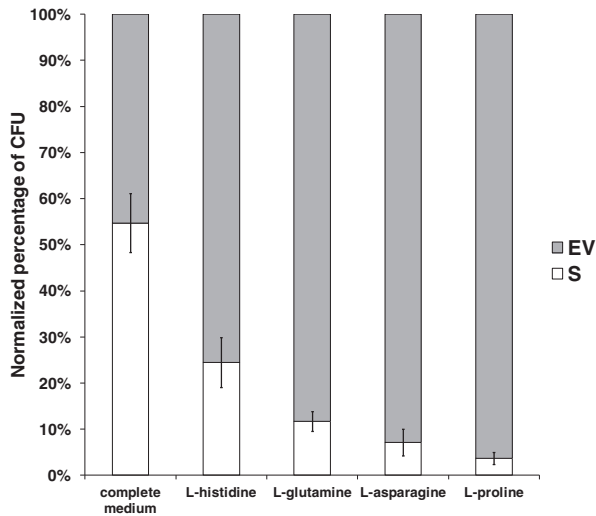


Fig. 6. The EV type provides fitness gain in specific environments. *In vitro* competition assay between the EV ($\Delta efpR$ - $\Delta efpH$) and S (WT) types inoculated at a 1:1 ratio in either complete medium or minimal medium supplemented with one amino acid as a sole carbon source. Competition experiments started with $\sim 5.10^5$ CFU ml⁻¹ and were stopped when cultures were above 10^9 CFU ml⁻¹. The percentage of CFU recovered was normalized by the percentage of CFU present in the inoculum. Two independent biological repeats, each comprising three technical repeats, were performed.

strain only reached a mean OD_{600nm} of 0.55 after 90 h (Fig. 7). This result confirmed that the growth rate of the EV type in minimal medium+ L-proline is significantly higher than the S type. The finding that growth of the culture inoculated with the $\Delta efpR$ -S type was much better than the WT culture, also suggested that this behaviour was dependent on the phenotypic heterogeneity occurring in the $\Delta efpR$ genetic background. To ascertain this hypothesis, we determined for each strain the percentage of EV type CFU in the inoculum and at the end of the exponential growth phase. In cultures inoculated with $\Delta efpR$ -EV type colonies, the percentage of EV type CFU was $69.9 \pm 11.3\%$ in the inoculum and reached $92.3 \pm 3.4\%$ at the end of the exponential growth phase (Fig. 7). For the cultures inoculated with the $\Delta efpR$ -S type, the percentage of EV type CFU was $1.6 \pm 0.3\%$ in the inoculum and reached $87.8 \pm 5.0\%$ at the end of the exponential growth phase. This analysis thus revealed that even a low percentage of EV cells in the *R. solanacearum* population allows the bacterial population to reach a higher cell density in this environment compared to a population exclusively composed of S cells (WT strain).

Phenotypic heterogeneity can be detected among natural *R. solanacearum* isolates

The *efpR* gene was originally discovered as a hotspot for adaptive mutations through serial passage experiments of *R. solanacearum* on host plants (Guidot *et al.*, 2014; Capela *et al.*, 2017). We investigated whether spontaneous

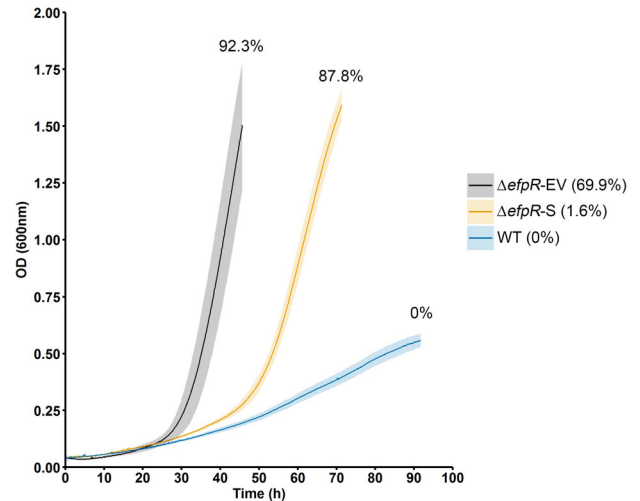


Fig. 7. Growth dynamic of $\Delta efpR$ -EV and -S types *in vitro*. Bacterial cultures were grown at 28°C in minimal medium supplemented with L-proline (20 mM), starting from a single colony of the EV ($\Delta efpR$) or S types (WT and $\Delta efpR$). The number in brackets represents the percentage of EV type CFU in the inoculum, whereas the percentage of EV type CFU at the end of the exponential growth phase is indicated above each growth curve. The dark lines represent the mean of three independent biological repeats and standard deviation is represented by the shaded region. Growth was monitored in microplates. Measurements were stopped at the end of the exponential growth phase.

mutations in *efpR* could also be identified when bacteria are grown *ex planta*. We found that spontaneous mutations in *efpR* occurred when *R. solanacearum* was maintained as a static culture in complete medium for 14 days. To ease the identification of such mutants, we used the GMI1000 strain transformed with a P_{RSc3148}-GFP construct because expression of RSc3148 is repressed by *efpR* (Capela *et al.*, 2017). The variants were then identified as fluorescent colonies and the *efpR* locus was sequenced to characterize the corresponding mutations. From two independent experiments, we identified 14 clones with a SNP in the *efpR* gene, corresponding to three distinct mutations. Two of them are non-synonymous mutations within the *efpR* coding sequence which, interestingly, were also detected after the *in planta* evolution experiment (same codon but different base substitution) (Fig. 8A). The third mutation occurred in the *efpR* promoter region, into the predicted -35 control element (Fig. 8A).

The observation that *efpR* variants arose *in planta* and *ex planta* and that both *efpR* and *efpH* are highly conserved in all *R. solanacearum* strains sequenced to date, prompted us to examine whether phenotypic heterogeneity could be a general feature of the *R. solanacearum* species complex (RSSC). We generated *efpR* deletion mutants in two phylogenetically distant strains: the Molk2 strain (*R. solanacearum*, phylotype IIB) and the Psi07 strain (*R. syzygii* subsp. *indonesiensis*, phylotype IV). Both Molk2 and Psi07 $\Delta efpR$ strains were phenotypically heterogeneous, with white fluidal colonies (S type) and dark red colonies (EV type) (Fig. 8B), similarly to what

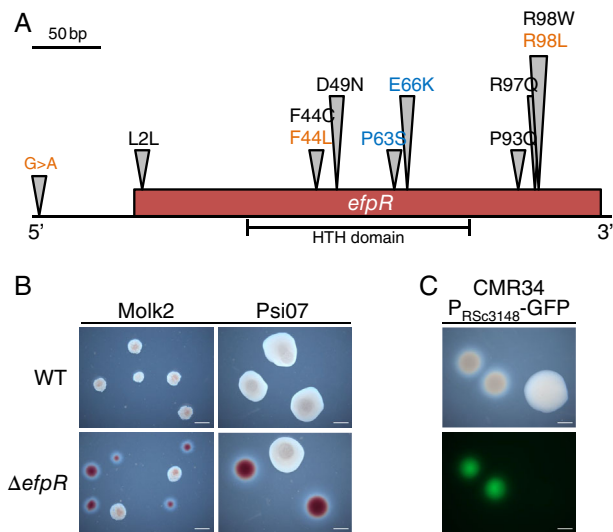


Fig. 8. The *efpR* gene is a hotspot for adaptive mutations, which generate phenotypic heterogeneity and lead to the emergence of EV type subpopulations among strains of the *R. solanacearum* species complex. (A) Schematic representation of the various mutations identified in *efpR* in three independent studies: in black, six mutations improving fitness of clones evolved in plant stems (Guidot *et al.*, 2014), in blue, two mutations improving plant infection (Capela *et al.*, 2017), and in orange, three mutations conferring fitness advantage in a static environment (this study). The region encoding the predicted helix-turn-helix (HTH) domain in EfpR is indicated. (B) Deletion of *efpR* in strains MolK2 and Psi07, taxonomically distant from GMI1000, also generates phenotypic heterogeneity. (C) Expression of the *RSc3148* promoter is specifically induced in EV-type colonies in strain CMR34. Bacteria were grown on complete medium agar plates for 52 h (B) or on minimal medium agar plates for 96 h (C). Scale bar = 2 mm.

was observed with strain GMI1000 (*R. pseudosolanacearum*, phylotype I).

The conservation of the *efpR*-mediated phenotypic heterogeneity phenomenon in phylogenetically distant strains suggested that EV type variants could be detected among natural RSC isolates. We screened a collection of 41 strains of the *R. solanacearum* species complex isolated worldwide and representative of the taxonomic diversity of this species complex (Prior *et al.*, 2016) (Table 1). We identified one *R. solanacearum* strain (CMR34, phylotype IIB) generating phenotypic heterogeneity stably over several subcultures on plate. This strain was transformed with the $P_{RSc3148}$ -GFP construct to determine whether the observed heterogeneity was *efpR*-dependent. Similarly to the GMI1000 strain, we observed EV colonies strongly expressing the reporter while it was not active in the S colonies (Fig. 8C). These results suggest that the *efpR*-dependent phenotypic switch can occur among natural isolates.

Discussion

In this study, we demonstrated that loss of function mutations in the global regulator EfpR generate phenotypic

heterogeneity in bacterial isogenic population of *R. solanacearum*. Indeed, *efpR* mutants always produced two types of colonies arising from a single clone, the type S ('smooth', similar to the WT) and the type EV ('*efpR* variant'). Both cell types have distinct phenotypic marks, highlighting that the S/EV switch phenomenon directly affects virulence and also drastically modifies bacterial cell physiology, especially by generating a form of metabolic heterogeneity in the population (Rosenthal *et al.*, 2018; Şimşek and Kim, 2018). The *efpR*-dependent molecular mechanism leading to the emergence of EV type cells remains to be discovered. Recently, downregulation of *efpR* was reported to be associated with three genes of unknown function, *RSc3146-3148*, two of which encoding proteins likely associated with the membrane (Capela *et al.*, 2017), and which are presumably associated with the S/EV transition. Our study shows that the neighbouring gene, *efpH* (*RSc3149*), plays a key role in this phenotypic switch. EfpH is a homologue of EfpR (79% identity), which also most probably operates as a transcriptional regulator. The *efpH* gene is not expressed in the WT strain; however, in the Δ *efpR* strain, *efpH* is one of the highest upregulated gene (Perrier *et al.*, 2016). Deletion of *efpH* did not generate phenotypic heterogeneity in the WT background, only forming S type colonies. On the other hand, the Δ *efpR*- Δ *efpH* double mutant also did not generate phenotypic heterogeneity but only formed EV type colonies. Both *efpR* and *efpH* are conserved in all the strains from the *R. solanacearum* species complex sequenced to date.

In a previous study, we showed that the *efpR* mutant had slightly reduced virulence when inoculated on tomato plants through soil drenching (Perrier *et al.*, 2016). Although the transcriptomic profiles of the Δ *efpR* and Δ *efpR*- Δ *efpH* mutants were mostly similar, the strength of the signal was stronger in the double mutant (more severe downregulation of the exopolysaccharide biosynthesis gene cluster, for example). This probably explains why the Δ *efpR*- Δ *efpH* double mutant (EV type) was strongly altered in pathogenicity on tomato plants compared to the WT (S type), while pathogenicity of the Δ *efpR* single mutant (EV + S types) was only mildly reduced. This suggested that the reduced disease severity on tomato plants observed for the Δ *efpR* single mutant results from the presence of EV cells in the population.

The finding that the Δ *efpR*- Δ *efpH* strain was stably 'locked' into the EV morphotype opened the way to test experimentally what is the adaptive gain for *R. solanacearum* to generate phenotypic heterogeneity. We first compared the individual fitness of EV and S cell types in different environments: the tomato plant stem, complete medium and minimal medium supplemented with different carbon sources. We found that the S type had better growth ability than the EV type into plant stem, whereas the EV type had better growth ability into minimal medium. In complete medium, the EV and S types had the same fitness. These results could support the hypothesis of a bet-hedging

Table 1. List of the WT strains of the *Ralstonia solanacearum* species complex investigated in this study and observation of phenotypic heterogeneity on complete BG medium.

Strain	Phylotype	Sequevar	Plant origin	Phenotypic heterogeneity
GMI1000	I	18	<i>Solanum lycopersicum</i>	–
TNT82A	I	14	<i>Solanum lycopersicum</i>	–
ACH92	I	116	<i>Zingiber officinale</i>	–
RUN0305	I	18	<i>Solanum lycopersicum</i>	–
TD1301	I	31	<i>Solanum melongena</i>	–
CIV23	I	31	<i>Solanum melongena</i>	–
RUN5501	I	31	<i>Solanum lycopersicum</i>	–
RUN3568	I	31	<i>Solanum lycopersicum</i>	–
RUN5536	I	18	<i>Solanum lycopersicum</i>	–
02–167	I	18	<i>Solanum lycopersicum</i>	–
RUN3573	I	14	<i>Solanum lycopersicum</i>	–
RUN5445	I	33	<i>Capsicum frutescens</i>	–
E'4 T2	I	47	<i>Solanum lycopersicum</i>	–
RUN5135	I	18	<i>Cyphostemma mappia</i>	–
T1-UY	IIA	50	<i>Solanum lycopersicum</i>	–
CFBP7054	IIA	52	<i>Solanum lycopersicum</i>	–
CFBP2958	IIA	39	<i>Solanum lycopersicum</i>	–
CFBP6779	IIA	38	<i>Canna indica</i>	–
CMR90	IIA	35	<i>Solanum lycopersicum</i>	–
Molk2	IIB	3	Banana	–
CMR34	IIB	1	<i>Solanum lycopersicum</i>	+
CIP417	IIB	3	Peanut	–
IBSBF2001	IIB	25	<i>Solanum lycopersicum</i>	–
RUN3733	III	19	<i>Solanum lycopersicum</i>	–
CMR15	III	29	<i>Solanum lycopersicum</i>	–
DGBBC1222	III	42	<i>Solanum tuberosum</i>	–
JT525	III	19	<i>Pelargonium asperum</i>	–
DGBBC1125	III	43	<i>Solanum tuberosum</i>	–
CMR66	III	49	<i>Solanum scabrum</i>	–
PSI07	IV	10	<i>Solanum lycopersicum</i>	–
RUN1308	IV	10	<i>Solanum lycopersicum</i>	–
ACH732	IV	11	<i>Solanum lycopersicum</i>	–
MAFF301558	IV	8	<i>Solanum tuberosum</i>	–
R229	IV	10	Banana	–
UQRS91	IV	10	<i>Solanum lycopersicum</i>	–
RUN1309	IV	10	<i>Solanum lycopersicum</i>	–
UQRS280	IV	10	<i>Solanum lycopersicum</i>	–
UQRS290	IV	10	<i>Solanum lycopersicum</i>	–
PSI36	IV	10	<i>Solanum lycopersicum</i>	–
UW522	IV	11	Clove	–
RUN4606	IV	10	<i>Solanum tuberosum</i>	–

strategy for *R. solanacearum* isogenic populations generating phenotypic heterogeneity with one part of the population expressing the S phenotype (virulent) better adapted to the plant environment while the other part expressing the EV phenotype is potentially better adapted to other environments such as minimal medium conditions. This also suggests that the generation of phenotypic heterogeneity in *R. solanacearum* population is certainly an advantageous strategy during the pathogen's lifecycle, which includes diversified environments (host plants, asymptomatic weeds, soil, watercourses, etc.).

In order to better understand the interaction between EV and S type cells, we also compared their fitness when co-inoculated in a same environment. Results indicated that the EV type is significantly more fit when co-inoculated with the S type than alone *in planta*. We demonstrated that the reactivation of EPS production in the EV type improves its

virulence, thus suggesting that the EV type could benefit from the EPS produced by the S type to improve its colonization and virulence *in planta*. However, our results also demonstrated that the S type is less fit *in planta* when co-inoculated with the EV type than alone. As the EV type has expanded metabolic capacities, we hypothesized that the EV type consumes the nutrients and divide faster, to the detriment of the S type, and in addition, does not pay the cost for EPS production and virulence (Peyraud *et al.*, 2016).

The *efpR* gene was originally discovered by characterizing mutations which appeared spontaneously in this gene after 300 generations of experimental evolution of *R. solanacearum* in the stem of different plants (Guidot *et al.*, 2014; Perrier *et al.*, 2016). Mutations in *efpR* were also reported to occur in strain GMI1000 when used to be experimentally evolved into a legume symbiont (Capela *et al.*, 2017). In this study, we also found that mutations in *efpR*

can be easily selected in stressing environments such as *in vitro* static cultures. This observation suggested that *efpR* variants might also exist in nature. A first argument supporting this view came from the careful analysis of a collection of WT strains, among which one of them presented the typical features of EV-S type subpopulations. Experimental testing of this hypothesis will require a specific sampling of the EV and S type colonies in the various natural environments inhabited by *R. solanacearum*.

This study highlights the potential significance of generating phenotypic heterogeneity in *R. solanacearum* isogenic populations as an adaptive strategy to changing environments, mediated by spontaneous mutations in the global regulator EfpR. Spontaneous mutations in another global regulator, PhcA, were also reported to generate avirulent but fast-growing phenotypic variants (Peyraud *et al.*, 2016; Khokhani *et al.*, 2017; Perrier *et al.*, 2018). However, *phcA* mutations generate a single phenotype and reversion of *phcA* mutants to the WT form certainly occurs at a very low frequency considering the nature of genetic alterations reported (Poussier *et al.*, 2003). Conversely, *efpR* mutations ensure that a mix of EV and S types are produced, thus maintaining a proportion of virulent population required to ensure efficient plant infection and eventually the ecological success of this pathogen. The impact of this phenotypic heterogeneity on pathogenicity opens new perspectives to tackle population dynamics underlying the bacterial wilt disease. Future sampling paying attention to EV type variants differing from the S type should provide a first estimate on the frequency of the *efpR*-mediated heterogeneity phenomenon in natural populations.

Experimental procedures

Bacterial strains, plant material and growth conditions

Ralstonia solanacearum strains used in this study are described in Table 1 and Supporting Information Table S3. Strains were grown in complete medium or in minimal medium at 28°C (Plener *et al.*, 2010). The pH of the minimal medium was adjusted to 6.5 with KOH. For agar plates, the complete medium was supplemented with D-glucose (5 g l⁻¹) and triphenyl tetrazolium chloride (0.05 g l⁻¹) and the minimal medium with sucrose (5 g l⁻¹) when necessary. The minimal medium was supplemented with carbon sources at 20 mM final concentration. When needed, antibiotics were added to the media at the following final concentrations (mg l⁻¹): spectinomycin, 40; gentamicin, 10; kanamycin, 50. Four-week-old tomato plants (*Solanum lycopersicum* var. SuperMarmande) were used for the inoculations. Plant experiments were conducted in a growth chamber under the following conditions: 75% humidity, 12 h light 28°C, 12 h darkness 27°C.

Transcriptome analysis

Total RNA was extracted from the WT GMI1000 strain, the Δ *efpR* mutant (GRS704) and the Δ *efpR*- Δ *efpH* double mutant (GRS908) growing in complete medium at comparable cell densities (OD_{600nm} = 0.5). Three biologically independent experiments were conducted for each strain. Total RNA extraction and ribosomal RNA depletion were performed as previously described (Perrier *et al.*, 2016; 2018).

Oriented paired-end RNA sequencing (2 × 125 bp) was carried out by Fasteris (Fasteris SA, Plan-les-Ouates, Switzerland), using an Illumina HiSeq 2500 instrument and the procedures recommended by Illumina, with adaptors and amplification primers designed by Fasteris. The size of selected inserts was 150–250 bp.

Mapping of the reads and statistical analysis were conducted as previously described (Perrier *et al.*, 2018). Between 0.69 and 3.86 millions of mapped read-pairs in coding sequences were obtained. Mapped reads were imported into the R environment. The package HTSFilter was used to eliminate very low expressed genes from the analysis. A total of 4930 genes out of the 5307 predicted genes were thus kept in. The R package DESeq2 was used to normalize and complete the differential analysis by conducting the built-in Wald test (Anders and Huber, 2010). The *p* values thus obtained were adjusted for multiple comparisons using the false-discovery rate (FDR) method (Strimmer, 2008). Genes with a FDR-adjusted *p* < 0.05 and an absolute Fold Change | FCI > 2 between strains were taken into consideration.

Construction of mutant strains and genetic constructs

Disruption of the *efpH* gene was performed by creating an unmarked gene deletion using *sacB*-mediated counter selection (Schäfer *et al.*, 1994). Briefly, upstream and downstream regions of *efpH* were PCR amplified using the primer pairs oAP35-36 and oAP37-38, respectively, and cloned into the *EcoRI*-*HindIII*-digested *pk18mobsacB* to generate *pk18-efpH* (Supporting Information Table S3). The circular *pk18-efpH* plasmid was inserted in the WT and Δ *efpR* strains by natural transformation (Perrier *et al.*, 2016). Kanamycin-resistant and sucrose-sensitive recombinant clones were first selected to launch an overnight culture in complete medium. In a second step, kanamycin-sensitive and sucrose-resistant clones were screened by PCR using the primer pair oAP33-34 to identify a Δ *efpH* recombinant.

To complement the Δ *efpR*- Δ *efpH* strain, a 1044 bp fragment was PCR-amplified using the primer pair oAP41-99 and cloned into the *Acc65I*-*BglII*-digested *pNP329* vector to generate *pNP329-efpH* (Supporting Information Table S3). The *pNP329-efpH* plasmid was linearized with *ScaI* before natural transformation.

To construct the strains expressing constitutively the *xpsR* gene, the *pNP329-P_{tac}-xpsR* plasmid was constructed. A

1051 bp fragment was PCR-amplified using the primers pair oAP171-176 and cloned into the *NdeI*-*BglII*-digested pNP329- P_{tac} (Supporting Information Table S3). The pNP329- P_{tac} -*xpsR* plasmid was linearized with *NheI* before natural transformation. Transformants were selected on gentamicin selective medium and checked by PCR using the primer pair oNP611-612.

Nucleotidic sequences of the primers used in this study are given in the Supporting Information Table S4. Construction of fluorescent strains using mCherry or GFP reporter constructs (Cruz *et al.*, 2013) for expression studies is detailed in the Supporting Information Material and Methods file 1.

Virulence tests

Sixteen tomato plants were inoculated by soil drenching with 500 ml of a 5×10^7 CFU ml⁻¹ bacterial suspension. Plant symptoms were scored daily using a disease-index scale ranging from 0 (no symptoms) to 4 (complete wilting) as previously described (Poueymiro *et al.*, 2009). Virulence assays were repeated three times for each strain. Disease scoring was transformed into binary data, with a disease index below 3 corresponding to 0 and a disease index equal to or higher than 3 corresponding to 1. This transformation was performed in order to construct survival curves and to apply the survival analysis statistical protocols (Machin *et al.*, 2006). Gehan–Breslow–Wilcoxon test was used to determine significant difference between strains using the Prism software (Prism, GraphPad, San Diego).

In planta competition assay

Two millilitres of each strains carrying different reporter fusions (GFPuv and mCherry) and grown overnight were centrifuged for 2 min at 17 000g. The pellet was resuspended in 2 ml of sterile water, and then diluted to 10^8 CFU ml⁻¹, mixed in equal proportion and diluted again to 10^6 CFU ml⁻¹. Competition was performed on 4-week-old tomato inoculated by stem injection with 10 μ l of the mixed inoculum, 1 cm above the cotyledons. After 3 days, 1 cm of stem was harvested 2.5 cm above the cotyledons, placed in a 2 ml centrifuge tube containing glass beads (2 mm diameter) and grinded during 1 min at 30 Hz with a mixer mill (MM 400, Retsch, Germany). Extracted bacteria were resuspended in 1 ml of sterile water, serial-diluted and plated on complete medium using an automatic spiral plater (easySpiral, Interscience, France). Green and red colonies were visualized and enumerated using a fluorescence stereo zoom microscope (Axio Zoom.V16, ZEISS, Germany). Three independent biological repeats were performed with 10–18 plants per repeats per conditions. Kruskal–Wallis and Dunn's multiple comparison tests were used to

establish statistical groups using the Prism software (Prism, GraphPad, San Diego).

In vitro competition assay

Bacteria were grown as described previously, except that the bacterial pellet was resuspended in 2 ml of either complete or minimal medium supplemented with the tested carbon source (20 mM final concentration). Bacterial cultures were diluted to 5×10^7 CFU ml⁻¹, mixed in equal proportion and diluted again to 5×10^5 CFU ml⁻¹ in a final volume of 15 ml. This volume was split in three independent test tubes of 5 ml and incubated at 28°C under shaking at 180 rpm until the culture reach OD_{600nm} > 1. Plating of bacteria and fluorescence detection was performed as described previously. Two independent biological repeats, each comprising three technical repeats, were performed.

Monitoring in vitro growth

Bacteria were grown overnight in complete liquid medium and plated in order to have isolated colonies. Single colonies (EV or S) were resuspended in minimal medium supplemented with L-Proline (20 mM) and diluted to 5×10^7 CFU ml⁻¹. An aliquot of 100 μ l was used to determine the initial proportion of EV and S CFU and 200 μ l was used as inoculum. Bacterial growth was monitored using a microplate spectrophotometer (FLUOstar Omega, BMG Labtech, Germany) during 91 h at 28°C under shaking at 700 rpm using a linear shaking mode. At the end of the exponential growth phase, 100 μ l was harvested for bacterial enumeration and fluorescence detection. Three independent biological repeats were performed.

In vitro static culture experiment

Glass haemolysis tubes were filled with 5 ml of complete medium and inoculated with a single colony of strain GMI1000 bearing the $P_{RSc3148}$ -GFP construct. After 14 days at 28°C without agitation, 10 μ l of the liquid surface was recovered, serial-diluted and plated on complete medium in order to have isolated colonies. Green fluorescent colonies were visualized as described above. The *efpR* locus of each purified clone was PCR-amplified with the primers oCBM2872-oAP77 and sequenced using primers oAP76 and oCBM2440 (Supporting Information Table S4). Five independent biological repeats were performed.

Acknowledgements

We thank Jean-Baptiste Ferdy, Alain Givaudan, Laurent Noël, Rémi Peyraud and Philippe Remigi for support and advices during the course of this work. Delphine Capela, Nemo Peeters and Laurent Deslandes for supplying

plasmids and/or primers. We also thank Patrick Barberis, Claire Benezech and Maëlys Puyo for technical assistance, and the Plateforme Imagerie from the Institut Fédératif de Recherche 3450. We acknowledge Richard Berthomé for the *R. solanacearum* strain collection used in this work, and Benoit Facon and Fabienne Vaillau for the observation of the colony morphotypes on plate of the CMR34 strain in La Réunion.

References

- Acar, M., Mettetal, J.T., and van Oudenaarden, A. (2008) Stochastic switching as a survival strategy in fluctuating environments. *Nat Genet* **40**: 471–475.
- Ackermann, M. (2015) A functional perspective on phenotypic heterogeneity in microorganisms. *Nat Rev Microbiol* **13**: 497–508.
- Anders, S., and Huber, W. (2010) Differential expression analysis for sequence count data. *Genome Biol* **11**: R106.
- Arnoldini, M., Vizcarra, I.A., Peña-Miller, R., Stocker, N., Diard, M., Vogel, V., et al. (2014) Bistable expression of virulence genes in salmonella leads to the formation of an antibiotic-tolerant subpopulation. *PLoS Biol* **12**: e1001928.
- Balaban, N.Q., Merrin, J., Chait, R., Kowalik, L., and Leibler, S. (2004) Bacterial persistence as a phenotypic switch. *Science* **305**: 1622–1625.
- Capela, D., Marchetti, M., Clérissi, C., Perrier, A., Guetta, D., Gris, C., et al. (2017) Recruitment of a lineage-specific virulence regulatory pathway promotes intracellular infection by a plant pathogen experimentally evolved into a legume symbiont. *Mol Biol Evol* **34**: 2503–2521.
- Casadesús, J., and Low, D.A. (2013) Programmed heterogeneity: epigenetic mechanisms in bacteria. *J Biol Chem* **288**: 13929–13935.
- Chai, Y., Chu, F., Kolter, R., and Losick, R. (2008) Bistability and biofilm formation in *Bacillus subtilis*. *Mol Microbiol* **67**: 254–263.
- Chin, C.Y., Tipton, K.A., Farokhyfar, M., Burd, E.M., Weiss, D.S., and Rather, P.N. (2018) A high-frequency phenotypic switch links bacterial virulence and environmental survival in *Acinetobacter baumannii*. *Nat Microbiol* **3**: 563–569.
- Cruz, A.P.Z., Ferreira, V., Pianzola, M.J., Siri, M.I., Coll, N. S., and Valls, M. (2013) A novel, sensitive method to evaluate potato Germplasm for bacterial wilt resistance using a luminescent *Ralstonia solanacearum* reporter strain. *Mol Plant Microbe Interact* **27**: 277–285.
- Diard, M., Garcia, V., Maier, L., Remus-Emsermann, M.N.P., Regoes, R.R., Ackermann, M., and Hardt, W.-D. (2013) Stabilization of cooperative virulence by the expression of an avirulent phenotype. *Nature* **494**: 353–356.
- Fraser, D., and Kaern, M. (2009) A chance at survival: gene expression noise and phenotypic diversification strategies. *Mol Microbiol* **71**: 1333–1340.
- Genin, S., and Denny, T.P. (2012) Pathogenomics of the *Ralstonia solanacearum* species complex. *Annu Rev Phytopathol* **50**: 67–89.
- Guidot, A., Jiang, W., Ferdy, J.-B., Thébaud, C., Barberis, P., Gouzy, J., and Genin, S. (2014) Multihost experimental evolution of the pathogen *Ralstonia solanacearum* unveils genes involved in adaptation to plants. *Mol Biol Evol* **31**: 2913–2928.
- Hallet, B. (2001) Playing Dr Jekyll and Mr Hyde: combined mechanisms of phase variation in bacteria. *Curr Opin Microbiol* **4**: 570–581.
- Harrison, F. (2013) Dynamic social behaviour in a bacterium: *Pseudomonas aeruginosa* partially compensates for siderophore loss to cheats. *J Evol Biol* **26**: 1370–1378.
- Huang, J., Carney, B.F., Denny, T.P., Weissinger, A.K., and Schell, M.A. (1995) A complex network regulates expression of *eps* and other virulence genes of *Pseudomonas solanacearum*. *J Bacteriol* **177**: 1259–1267.
- Khokhani, D., Lowe-Power, T.M., Tran, T.M., and Allen, C. (2017) A single regulator mediates strategic switching between attachment/spread and growth/virulence in the plant pathogen *Ralstonia solanacearum*. *MBio* **8**: e00895–e00817.
- Machin, D., Cheung, Y.B., and Parmar, M. (2006) *Survival Analysis: A Practical Approach*, 2nd edn. Oxford, UK: Wiley, pp, 278.
- Mansfield, J., Genin, S., Magori, S., Citovsky, V., Sriariyanum, M., Ronald, P., et al. (2012) Top 10 plant pathogenic bacteria in molecular plant pathology. *Mol Plant Pathol* **13**: 614–629.
- Mouammine, A., Pages, S., Lanois, A., Gaudriault, S., Jubelin, G., Bonabaud, M., et al. (2017) An antimicrobial peptide-resistant minor subpopulation of *Photobacterium luminescens* is responsible for virulence. *Sci Rep* **7**: 43670.
- Peeters, N., Guidot, A., Vaillau, F., and Valls, M. (2013) *Ralstonia solanacearum*, a widespread bacterial plant pathogen in the post-genomic era. *Mol Plant Pathol* **14**: 651–662.
- Perrier, A., Barlet, X., Peyraud, R., Rengel, D., Guidot, A., and Genin, S. (2018) Comparative transcriptomic studies identify specific expression patterns of virulence factors under the control of the master regulator PhcA in the *Ralstonia solanacearum* species complex. *Microb Pathog* **116**: 273–278.
- Perrier, A., Peyraud, R., Rengel, D., Barlet, X., Lucasson, E., Gouzy, J., et al. (2016) Enhanced in planta fitness through adaptive mutations in EfpR, a dual regulator of virulence and metabolic functions in the plant pathogen *Ralstonia solanacearum*. *PLoS Pathog* **12**: e1006044.
- Peyraud, R., Cottret, L., Marmiesse, L., and Genin, S. (2018) Control of primary metabolism by a virulence regulatory network promotes robustness in a plant pathogen. *Nat Commun* **9**: 418.
- Peyraud, R., Cottret, L., Marmiesse, L., Gouzy, J., and Genin, S. (2016) A resource allocation trade-off between virulence and proliferation drives metabolic versatility in the plant pathogen *Ralstonia solanacearum*. *PLoS Pathog* **12**: e1005939.
- Plener, L., Manfredi, P., Valls, M., and Genin, S. (2010) PrhG, a transcriptional regulator responding to growth conditions, is involved in the control of the type III secretion system regulon in *Ralstonia solanacearum*. *J Bacteriol* **192**: 1011–1019.
- Poueymiro, M., Cunnac, S., Barberis, P., Deslandes, L., Peeters, N., Cazale-Noel, A.-C., et al. (2009) Two type III secretion system effectors from *Ralstonia solanacearum* GMI1000 determine host-range specificity on tobacco. *Mol Plant-Microbe Interact* **22**: 538–550.

- Poussier, S., Thoquet, P., Trigalet-Demery, D., Barthet, S., Meyer, D., Arlat, M., and Trigalet, A. (2003) Host plant-dependent phenotypic reversion of *Ralstonia solanacearum* from non-pathogenic to pathogenic forms via alterations in the *phcA* gene. *Mol Microbiol* **49**: 991–1003.
- Prior, P., Ailloud, F., Dalsing, B.L., Remenant, B., Sanchez, B., and Allen, C. (2016) Genomic and proteomic evidence supporting the division of the plant pathogen *Ralstonia solanacearum* into three species. *BMC Genomics* **17**: 90.
- Rainey, P.B., Beaumont, H.J., Ferguson, G.C., Gallie, J., Kost, C., Libby, E., and Zhang, X.-X. (2011) The evolutionary emergence of stochastic phenotype switching in bacteria. *Microb Cell Fact* **10**: S14.
- Ronin, I., Katsowich, N., Rosenshine, I., and Balaban, N.Q. (2017) A long-term epigenetic memory switch controls bacterial virulence bimodality. *eLife* **6**: e19599.
- Rosenthal, A.Z., Qi, Y., Hormoz, S., Park, J., Li, S.H.-J., and Elowitz, M.B. (2018) Metabolic interactions between dynamic bacterial subpopulations. *eLife* **7**: e33099.
- Rufián, J.S., Macho, A.P., Corry, D.S., Mansfield, J.W., Ruiz-Albert, J., Arnold, D.L., and Beuzón, C.R. (2018) Confocal microscopy reveals in planta dynamic interactions between pathogenic, avirulent and non-pathogenic *Pseudomonas syringae* strains. *Mol Plant Pathol* **19**: 537–551.
- Rufián, J.S., Sánchez-Romero, M.-A., López-Márquez, D., Macho, A.P., Mansfield, J.W., Arnold, D.L., *et al.* (2016) *Pseudomonas syringae* differentiates into phenotypically distinct subpopulations during colonization of a plant host. *Environ Microbiol* **18**: 3593–3605.
- Schäfer, A., Tauch, A., Jäger, W., Kalinowski, J., Thierbach, G., and Pühler, A. (1994) Small mobilizable multi-purpose cloning vectors derived from the *Escherichia coli* plasmids pK18 and pK19: selection of defined deletions in the chromosome of *Corynebacterium glutamicum*. *Gene* **145**: 69–73.
- Schreiber, F., Littmann, S., Lavik, G., Escrig, S., Meibom, A., Kuypers, M.M.M., and Ackermann, M. (2016) Phenotypic heterogeneity driven by nutrient limitation promotes growth in fluctuating environments. *Nat Microbiol* **1**: 16055.
- Şimşek, E., and Kim, M. (2018) The emergence of metabolic heterogeneity and diverse growth responses in isogenic bacterial cells. *ISME J* **12**: 1199–1209.
- Stewart, M.K., Cummings, L.A., Johnson, M.L., Berezow, A. B., and Cookson, B.T. (2011) Regulation of phenotypic heterogeneity permits salmonella evasion of the host caspase-1 inflammatory response. *Proc Natl Acad Sci U S A* **108**: 20742–20747.
- Strassmann, J.E. (2000) Evolution: bacterial cheaters. *Nature* **404**: 555–556.
- Strimmer, K. (2008) A unified approach to false discovery rate estimation. *BMC Bioinformatics* **9**: 303.
- Tuchscher, L., Medina, E., Hussain, M., Völker, W., Heitmann, V., Niemann, S., *et al.* (2011) *Staphylococcus aureus* phenotype switching: an effective bacterial strategy to escape host immune response and establish a chronic infection. *EMBO Mol Med* **3**: 129–141.
- Veening, J.-W., Smits, W.K., and Kuipers, O.P. (2008) Bistability, epigenetics, and bet-hedging in bacteria. *Annu Rev Microbiol* **62**: 193–210.
- Weigel, W.A., and Dersch, P. (2018) Phenotypic heterogeneity: a bacterial virulence strategy. *Microbes Infect* **20**: 570–577.
- Workentine, M.L., Sibley, C.D., Glezerson, B., Purighalla, S., Norgaard-Gron, J.C., Parkins, M.D., *et al.* (2013) Phenotypic heterogeneity of *Pseudomonas aeruginosa* populations in a cystic fibrosis patient. *PLoS One* **8**: e60225.

Supporting Information

Additional Supporting Information may be found in the online version of this article at the publisher's web-site:

Appendix S1: Supplementary-Material.

Figure S1. Observation of phenotypic heterogeneity in *Ralstonia solanacearum* GMI1000 Δ *efpR* and *efpR* SNP mutants obtained after experimental evolution in planta. Colonies formed after 52 h at 28°C on complete medium agar plates supplemented with D-glucose and triphenyl tetrazolium chloride red are observed under a stereo-microscope. Black arrows indicate less mucoid colonies compared to the GMI1000 wild-type (WT) colonies, with a red center and layered edge. Δ *efpR::efpR* and Δ *efpR::\Delta**efpH::efpH* are the *efpR* and *efpH* complemented strains, respectively. *efpR*^{P93Q}, *efpR*^{L2L} and *efpR*^{D49N} are the *in planta* evolved *efpR* SNP mutants. Scale bar = 2 mm.

Figure S2. Differential expression pattern of the *fliC* promoter in S and EV type colonies. Left panels show bright field images; the right panels show the same colonies under fluorescence excitation. For the Δ *efpR* strain, one type EV (left) and one type S (right) colonies are shown. Expression of the P_{fliC}-mCherry reporter occurs only in EV type colonies. Bacteria were grown on BG agar plates for 52 h at 28°C. Scale bar = 2 mm.

Figure S3. Comparison of the *fliC* promoter activity in *R. solanacearum* GMI1000 wild-type (WT), Δ *efpR* and Δ *efpR::\DeltaefpH* populations after overnight growth in complete liquid medium.** To visualize *R. solanacearum* cells, overnight cultures in complete liquid medium were diluted ten times and 4 μ l was mounted between a 1 mm 1% agarose pad on a microscope slide and a cover slip. Bacteria were imaged using a Leica TCS SP8 confocal laser microscope, with a 40x water objective and the LAS X software (Leica).

Left panels show bright field images of the 3 different strains, the middle panels show eGFP fluorescence profile of the 3 strains and the right panels show the overlay of the two first panels. In the WT strain, the *fliC* promoter is weakly active in all the cells while in the Δ *efpR* strain, the promoter is weakly active in a subpopulation (white arrows) and an other subpopulation the promoter is strongly active. In the Δ *efpR::\Delta**efpH* strain the *fliC* promoter is strongly active in most of the cells, a few cells per field show low activity pattern. Scale bar = 10 μ m.

Figure S4. Impact of the initial ratio of the EV and S types on the *in planta* fitness of the population. Bacteria were co-injected in tomato stems at various initial ratio (100:0, 99:1, 90:10, 50:50, 10:90) and harvested 3 days post-inoculation. The strain represented is

indicated in bold while the co-inoculated strain is indicated in brackets. Three independent biological repeats were performed with 5 to 8 plants per repeats per conditions. Bars indicate standard deviation.

Table S1. RNAseq data for all wild-type GMI1000 strain, $\Delta efpR$ mutant (GRS704) and $\Delta efpR$ - $\Delta efpH$ double mutant (GRS908) transcripts detected in complete medium.

Table S2. Differentially expressed genes (DEG) between the WT GMI1000 strain and the $\Delta efpR$ mutant or the $\Delta efpR$ - $\Delta efpH$ double mutant, or between $\Delta efpR$ mutant and the $\Delta efpR$ - $\Delta efpH$ double mutant in complete medium.

Table S3. List of strains and plasmids used and constructed in this study.

Table S4. List of primers used in this study.